The performance of Borehole Heat Exchanger installed in unsaturated soils

Fujiao Tang, Hossein Nowamooz
ICUBE, UMR 7357, CNRS, INSA de Strasbourg, 24 boulevard de la Victoire, 67084 Strasbourg
fujiao.tang@insa-strasbourg.fr

Keywords: Borehole Heat Exchanger, unsaturated soil, heat pump performance.

ABSTRACT

This paper studied the hydrothermal behavior of unsaturated soils as surrounding media for the shallow installed Borehole Heat Exchanger (BHE). Under seasonal environmental solicitations on the soil surface, the soil hydrothermal properties vary with time and space in the shallow zone. Appropriate models for hydrothermal transfer in porous media were implemented in the numerical framework to investigate the performance of a heat pump coupled with the BHE considering different surrounding soils (clay, sandy loam and sand). The results showed that soil thermal properties vary in different soils due to their unique water retaining capabilities, resulting to the different performance of the BHE. It was concluded that the BHE installed in sand and sandy loam had a better performance than that installed in clay. However, the BHE installed in sandy loam and sand had insignificant difference of performance between each other.

1. INTRODUCTION

Geothermal energy is a clean and environmental-friendly energy. According to Saner et al. (2010), using borehole heat exchanger (BHE) instead of methane furnaces decreases the CO_2 emissions by up to 84%. Advantages of BHE also include an elevated level of comfort (low noise) and low running cost (Bandos et al., 2009). However, the installation cost of BHE is more compared with conventional heat exchangers. Recently, the focus is in on the optimization of the system to save energy (Zhang et al, 2016).

Right now, there are mainly two usages of geothermal energy, to generate electricity and to provide heat. The depth of a geothermal well should be long enough to generate electricity. While it is much easier to provide heat with less depth (20 - 300 m). Radioti et al. (2017) have reported that short BHEs (length < 40 m) are economically advantageous compared to long BHEs in urban areas. Compared with Horizontal Ground Heat Exchanger (HGHE), BHE is more popular because it has less space requirement. Moreover, it is less influenced by the seasonal temperature fluctuations (Florides et al., 2007; Molina-Giraldo et al., 2011; Hu, 2017). Sanner et al. (2003) have specified that vertical BHE shows better performance and energy efficiency than HGHE. Compared to a closed-loop system, the open-loop system has a higher energy yield, while they have a higher environmental risk due to the water pollution (Cui et al., 2016). For shallow boreholes, the most often used closed-loop pipe type is U-tube (Sliwa and Rosen. 2015).

Although there are a lot of studies on BHE treating their experimental aspects, their analytical solutions and their numerical modeling validations, few studies have considered the hydrothermal variations in the unsaturated soils. The soil surface is influenced not only by the seasonal temperature variations but also periodical hydraulic solicitations (or suction variations). The suction has the advantage to represent the water flow in the horizontal direction. In addition, the suction range is known based on the existing field measurements and laboratory tests.

It has been recognized in the literature that the thermal properties are sensitive to water content (Abu-Hamdeh, 2000). The seasonal suction variations modify the water content and consequently the soil thermal properties (Hydrothermal coupling). Although the depth of moisture variations is around 1.5 m to 2.0 m, the temperature variations can reach around 10 m below surface. Rivera et al. (2015) report that the ground surface supplies up to 35% of the energy for a BHE. Mikhaylova et al. (2016) and Hein et al. (2016) report that BHE depth is significantly influenced by the thermal conductivity of surrounding soil. Zhang et al. (2015) indicate that the soil thermal properties have a close relationship with the temperature around a BHE.

There are mainly three computational methods in studying BHE: analytical method (Zeng et al, 2003; Rivera et al., 2015; Li et al., 2012; Javed and Spitler, 2017), semi-analytical method (Claesson and Eskilson, 1988), and numerical method (Lee and Lam, 2008; Liu, et al., 2019). Analytical models are mostly based on Kelvin's point source theory. For the infinite cylindrical and line source model, points are assumed along a line in a domain, and the constant heat load is assumed. They are solved analytically by using Laplace transformation, Bessel equation, etc. The finite line source model presumes the domain as a semi-infinite domain (Carslaw and Jaeger, 1959). By employing the finite line source method, Claesson and Eskilson (1988) have developed a dimensionless G-function, which is a combination of the analytical and numerical method. After that, many models have been developed, including a short-time response model (Larmarche and

Beauchamp, 2007) and a transient analytical model using spectral analysis (Al-Khoury, 2010). The analytical and semi-analytical methods are time-saving and simplified computation methods based on assumptions on soil layers, boundaries, etc. (Al-Khoury et al., 2005). Moreover, most of the analytical models ignore the hydrothermal variations in soil. Bidarmaghz et al. (2016) conclude that a depth reduction of 11% can be saved for a 30 m BHE considering the surface thermal recharge. Conventionally, the analytical models ignore the heat transfer in the axial direction. Marcotte (2011) declares that borehole length is 15% shorter when axial conduction effects are considered.

In this context, a finite element model (FEM) has been built to distinguish the influence of soil media on the performance of a shallow installed BHE by considering the unsaturated soil behavior. The model regarded the pipe and its carrying fluid as a 1d material, while the grout and the surrounding soils were considered as a 3D material.

2. EQUATIONS USED IN THE MODEL

The model contained the following parts: the water transfer in unsaturated soils, the soil thermal properties, the heat transfer in the pipe, the heat transfer in concrete (grout), the heat transfer in porous media, as well the approach to investigating the performance of heat pump.

2.1 Water transfer equation in unsaturated soil

Water in porous media is regarded to be incompressible and there is no mass transfer of soil particles. The water vapor was not considered since it was not significant in our calculations.

The Darcy velocity in unsaturated soils is given as:

$$\mathbf{u} = -\mathbf{K} \cdot k_r \cdot \nabla\left(H_p + H_k + D\right) \quad [1]$$

where, K is hydraulic conductivity (m/s) of porous media, k_r is relative hydraulic conductivity, H_p is water potential or suction head (m), H_k is the kinetic head (m), D is elevation head (m). In our model, the kinetic head was very small and was ignored. Mualem equation (1976) was used for the calculation of relative hydraulic conductivity k_r:

$$k_r = \begin{cases} S_e^{\,l}\left[1-\left(1-S_e^{\,n/(n-1)}\right)^m\right]^2 & H_p < 0 \\ 1 & H_p \geq 0 \end{cases} \quad [2]$$

where, m is defined as:

$$m = 1 - 1/n \quad [3]$$

and the relative saturation Se is computed as:

$$S_e = \frac{\theta - \theta_r}{\theta_s - \theta_r} \quad [4]$$

In the above equations, l is pore conductivity parameter, n and m are constant parameters, θ_s and θ_r are saturated volumetric water content and residual volumetric water content.

van Genucheten (1980) equation is used for the calculation of suction and relative saturation:

$$S_e = \begin{cases} \dfrac{1}{\left[1+\left|\alpha H_p\right|^n\right]^{1-1/n}} & H_p < 0 \\ 1 & H_p \geq 0 \end{cases} \quad [5]$$

where, α (m^{-1}) is Van Genucheten parameter.

Richards equation (1931) is applied to calculate the variation of water potential with time and space, expressed as:

$$\rho \cdot \mathrm{C} \cdot \frac{\partial H_p}{\partial t} + \nabla \cdot \left[-K \cdot k_r \cdot \nabla \cdot \rho \cdot \left(H_p + D\right)\right] = 0 \quad [6]$$

where, C is specific moisture capacity representing the amount of water that the soil can hold at a specific suction (1/m).

2.2 Soil thermal properties

In this investigation, the approach proposed by Nowamooz et al. (2015) for the thermal conductivity is used in the numerical simulation model:

$$k = (k_{sat} - k_{dry})\,k_e + k_{dry} \quad [7]$$

where,

$$k_{sat} = 0.53x_s + 0.1\gamma_d \quad [8]$$

$$k_{dry} = 0.087x_s + 0.019\gamma_d \quad [9]$$

$$k_e = \frac{\kappa S_r}{1 + (\kappa - 1)\,S_r} \quad [10]$$

In the above equations, S_r is the soil saturation; x_s is the gravimetric sand content; γ_d is the soil dry density multiplied by gravity (kN.m^{-3}), κ is the particle factor proportional to sand content.

Tang and Nowamooz model (2018) is used to obtain soil volumetric heat capacity:

$$C_v = (C_{sat} - C_{dry})\,S_r + C_{dry} \quad [11]$$

with the dry and saturated volumetric heat capacity C_{dry} and C_{sat} expressed as:

$$C_{dry} = 1.2\rho_d - 0.5x_s \quad [12]$$

$$C_{sat} = 4.18 - 0.05\rho_d - 0.75x_s \quad [13]$$

where, ρ_d is dry density (g.cm^{-3}).

2.3 Heat transfer in pipe

The 1D heat transfer in the pipe includes its wall layer, its internal film, and the carrying incompressible fluid. The Energy balance in U-tube can be then represented in the following form:

$$\rho_f AC_{p-f}\frac{\partial T_f}{\partial t} + \rho_f AC_{p-f}\mathbf{u}_f \cdot \nabla T_f = \nabla \cdot Ak_f \nabla T_f + f_D \frac{\rho_f A}{2d_h}\mathbf{u}_f \mathbf{u}_f{}^2 + Q_f + Q_{film-f} \quad [14]$$

where, ρ_f is the fluid density (kg/m3), A is the pipe cross-sectional area (m^2), C_{p-f} is the fluid specific heat capacity (J/(kg.K)), T_f is the fluid temperature, u_f is the flowing velocity of fluid (m/s), k_f is the fluid thermal conductivity W/(m.K), f_D is the Darcy friction factor, d_h is the hydraulic diameter (m), Q_f represents the heat source (W/m), Q_{film-f} indicates the energy absorbed (extracted) through internal film (W/m).

The energy transfer by convection is:

$$Q_{film-f} = (\mathrm{hZ})_{eff}(\mathrm{T}_{fo} - \mathrm{T}_f) \quad [15]$$

where,

$$h = Nu\frac{k_f}{d_h} \quad [16]$$

The energy difference between outside and inside layer is:

$$Q_{c-wall} = \frac{2\pi\Delta L k_p}{\ln(r_{out}/r_{in})}(\mathrm{T}_c - \mathrm{T}_{fo}) \quad [17]$$

where, L is the pipe length, r_{out} and r_{in} are the outside and inside radius of pipe, T_c is the temperature of exterior wall layer.

2.4 Heat transfer in grout

Heat transfer in the grout (concrete) is presumed by the conduction. The energy transfer equation regarding the surrounding concrete lining is:

$$\rho_g C_{p-g}\frac{\partial T_g}{\partial t} = \nabla \cdot (k_g \nabla T_g) + Q_g \quad [18]$$

where, ρ_g, C_{p-g}, T_g, k_g are respectively the density (kg/m^3), heat capacity (J/(kg.K)), temperature (K), and thermal conductivity (W/(m.K)) of the concrete lining, Q_g is the heat source (W/m^3).

2.5 Heat transfer in porous soil

Heat balance equation in soil can be represented by:

$$\rho_s C_s\frac{\partial T_s}{\partial t} = \nabla \cdot (k_s \nabla T_s) + \nabla \cdot (\rho_f C_{p-f}\mathbf{u}_f T_s) + Q_s \quad [19]$$

where, ρ_s is the soil density (kg/m^3), T_s is temperature, t is time, k_s is the soil thermal conductivity (w/(m.K)), C_s is the soil heat capacity (J/(kg.K)), ρ_f is the fluid density in soil (kg/m^3), A is the cross-sectional area of water flow (m^2), C_{p-f} is the fluid heat capacity (J/(kg.K)), u_f is the fluid velocity in soil (m/s), Q_s is the heat source (W/m^3).

2.6 Approaches to investigating heat pump Coefficient of Performance (COP) and Total Extracted Energy (TEE)

For the heating process, many researchers (Hein et al., 2016; Shao et al., 2016; Casasso et al., 2014; Sanner et al., 2003) have pointed out that the heat pump COP can be treated as a linear function of the outlet temperature:

$$COP = aT_{out} + b \quad [20]$$

The coefficients a and b are taken 0.1452 ($°C^{-1}$) and 4.0298 respectively (Glen Dimplex Deutschland GmbH, 2016).

The following equation is used for the TEE in the numerical simulations:

$$\frac{d_{Q_{ext}}}{d_t} = A\rho_f u_f C_{p-f}(T_{out} - T_{in}) \quad [21]$$

where, Q_{ext} represents extracted energy (J), t is time (s), A indicates the sectional area of U-tube (m^2), ρ_f is fluid density (kg/m^3), u_f is fluid velocity (m/s), C_{p-f} is fluid specific capacity (J/(kg.K)).

3 MODEL DESCRIPTIONS

In this part, the geometry mesh, the necessary parameters, the hydrothermal conditions applied on the top and bottom boundaries, the initial hydrothermal profile of the surrounding soils, and the operation options of the BHE were described for the numerical simulations.

3.1 Model geometry and mesh

The studied model was supposed to be a 3D model with a side length of 30 m and a depth of 100 m (Figure 1-a). The height was constituted of two parts: 30 m of soils on the top and 70 m of claystone (bedrock) on the bottom. The grout surrounding the single U-tube was supposed to be with a height of 25 m and the U-tube was with the depth of 20 m. The diameter of borehole was 0.14 m. Inside the borehole, the U-tube was symmetrically installed. The inner and outer diameter of U-pipe was 2.2 cm and 2.5 cm. The mesh used in the numerical simulations was also presented in Figure 1-b.

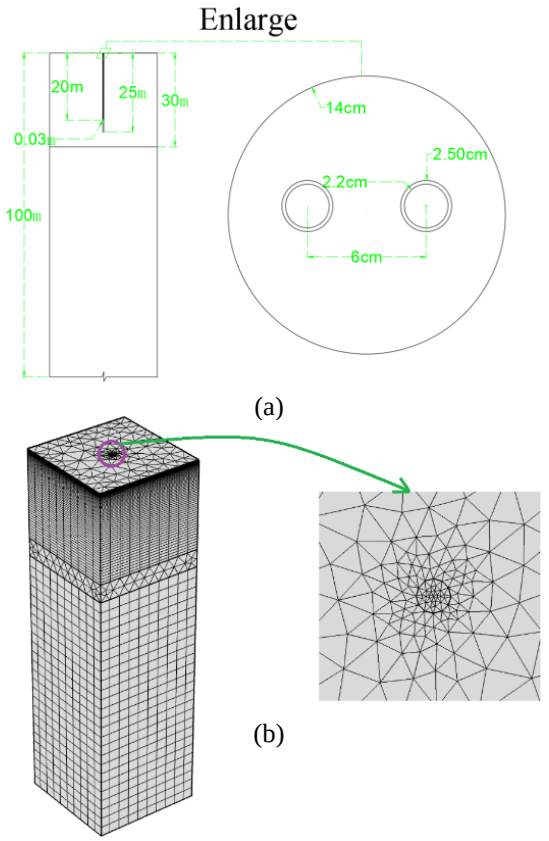

Figure 1: (a) Schematic geometry for BHE and its surrounding soil; (b) mesh used in the numerical modelling.

3.2 Parameters used in the numerical simulations

Three typical soils (sand, sandy loam and clay) were considered in this study. Table 1 summarized the main hydrothermal properties of the soils surrounding the BHE. Where, ρ_s was the specific soil density.

A pure water was chosen as the carrying fluid since no negative temperature was considered in the simulations. The U-tube was a high-density polyethylene pipe (HDPE) with a high durability and strength (Florides et al., 2007). Grout was used as a surrounding material of the U-pipe.

3.3 Initial hydrothermal boundary conditions

Seasonal suction and temperature conditions were only imposed on the soils surface (Dirichlet boundary) for a period of 365 days (1 year). A mild climate for thermal condition and a grass field for the hydraulic condition were respectively applied with the following equations.

$$T_{top} = -30 \cdot \left[\sin(pi/365 \cdot t) - 1\right] \quad [22]$$

$$S_{top} = -1.99 \cdot \left[\sin(pi/365 \cdot t) - 1\right] + 0.01(MPa) \quad [23]$$

No water and heat flow (out or in) was imposed to the left, right and bottom boundaries. The temperature gradient on the bottom of geometry was taken equal to 0 °C/m.

3.4 Initial hydrothermal profiles

An equilibrium method (Tang and Nowamooz, 2018) has been used to obtain the initial hydrothermal profiles. After several cycles, an equilibrium stage could be reached with the negligible difference in the suction or temperature profiles for the last final cycles. This hydrothermal equilibrium stage was used as the initial profile in this work. The initial suction profile for a grass field and the initial temperature profile for a mild climate condition were shown in Figure 2.

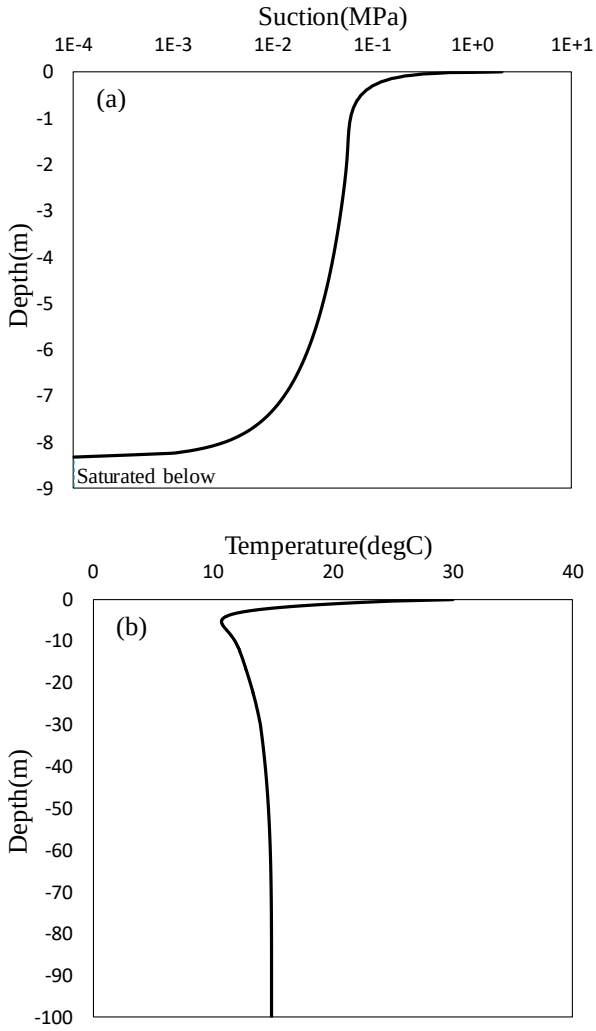

Figure 2: Initial hydrothermal profiles: (a) initial suction (Pa); (b): initial temperature (°C).

3.5 Operation options

When the temperature on the top surface was lower than 10°C, the BHE would start working. On the contrary, when the temperature on the top surface was higher than 10 °C, the BHE would stop working. According to the imposed meteorological conditions on the soil surface (equation [22]), BHE operated for 196 days per year for T_{on}=10 °C.

4 Numerical simulation results

As the numerical simulation framework has been validated in literatures (Tang and Nowamooz, 2018; Tang and Nowamooz, 2019), the numerical simulation

results concerning current investigation would be brought out followingly.

4.1 Variation of hydrothermal properties with time and space for sandy loam soil

With the seasonal hydraulic conditions imposed on the top surface, the soil suction changed with time and space according to Darcy equation, Richards equation (1931), Mualem equation (1976), and van Genucheten equation (1980) (Figure 3).

By using equations [7-10] and [11,12,13], the seasonal variations of the soil thermal conductivity and the soil volumetric heat capacity can be estimated with time and space.

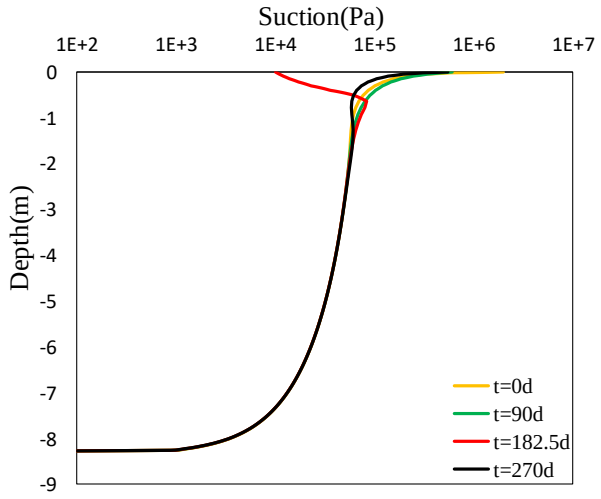

Figure 3: Hydrothermal properties in porous media: (a) suction; (b) volumetric water content; (c) soil thermal conductivity; (d) soil volumetric heat capacity.

4.2 Influence of the 3 soil types on heat pump COP

Three different soils were studied in this part: sand, loamy sand and clay. Figure 4 showed the variation of the thermal conductivity of the different soil with time and space. The thermal conductivity of sand had the largest variation while that of clay had the least variation. In saturated condition, the sand had the biggest thermal conductivity.

By analyzing the variation of the soil thermal conductivity after 3 and 6 months (Figure 5), we found that the thermal conductivity of sandy loam and sand was higher than that of clay soil in the saturated and unsaturated zones. Sand had the greatest thermal conductivity in the saturated zone and the thermal conductivity for sandy loam was the greatest in the unsaturated zone.

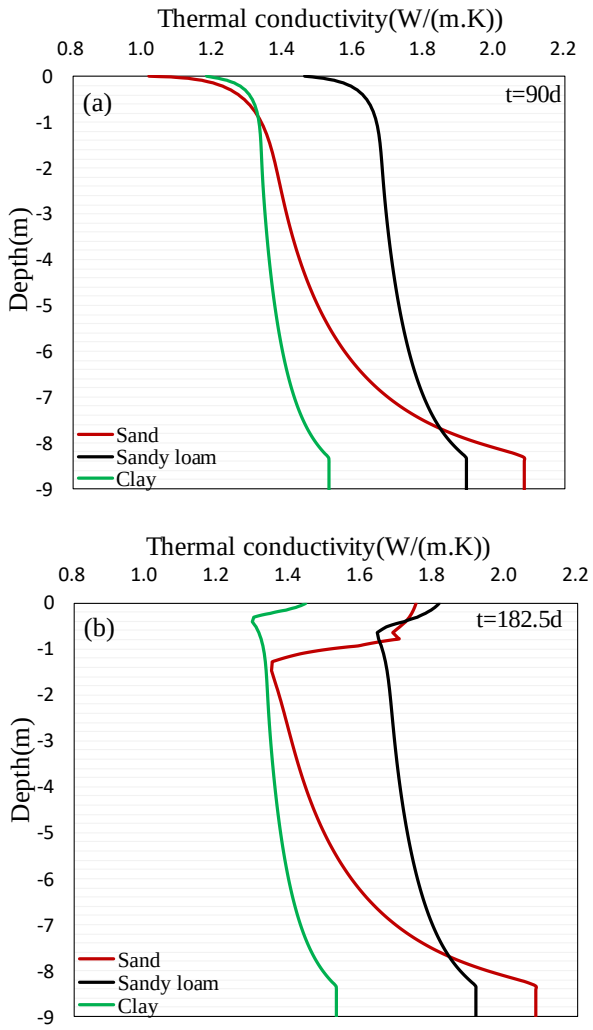

Figure 5: Thermal conductivity for 3 soils with time: (a) 3 months; (b) 6 months.

TEE and the heat pump COP of BHE installed in three different soils were exploited during 1 year (Figure 6). It could be concluded that the extracted TEE for sandy loam soil and sand was 12.8% and 12.4% more energy than that of clay (Figure 6-a). With the decrease of the surface temperature during the cold seasons, the COP at first decreased dramatically and it reached its minimum value after 222 days (Figure 6-b). Then, it increased with the increase of the surface temperature. In the sand and sandy loam, the COP values were very close (negligible difference), and higher than those of clay.

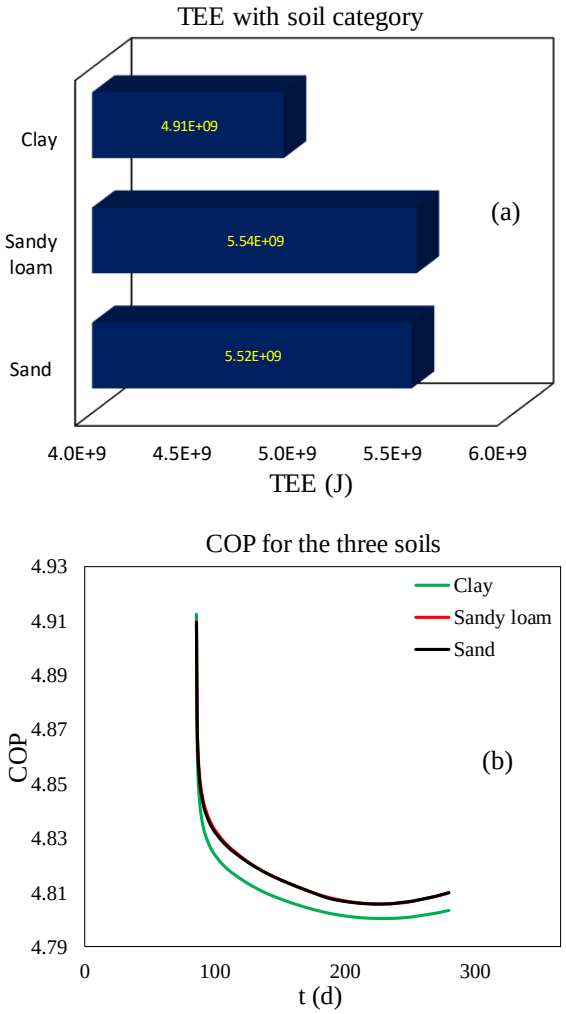

Figure 6: The operation of the BHE after one year for three soils: (a) TEE; (b) heat pump COP.

5 CONCLUSION

In this work, unsaturated soils were chosen as the surrounding medias for BHE. Appropriate models for the soil water retention curve, the soil thermal conductivity and the volumetric heat capacity were implemented simultaneously in the numerical framework. The initial suction and temperature value with depth were deliberately chosen to be in an equilibrium state.

It was found that the variation of temperature profile and water content corresponded to the existing analytical solution. BHE performance considering geotechnical condition was investigated in the numerical modelling. It was concluded that the BHE installed in sand and sandy loam extracted 12.4% and 12.8% more energy than that in clay. While there was negligible performance for the BHE installed in sandy loam and sand.

The investigation has provided a view for how soil properties can change soil thermal properties in different soils, and thus affect the BHE performance. The investigation furthermore helps to understand better the technical mechanism for BHE installed in soils.

Table 1 Hydrothermal properties of the studied soils

Material	χ_s	K (m/s)	l	α (m^{-1})	n	θ_s	θ_r	ρ_s (g/cm3)	ρ_d (g/cm^3)
Sand	0.9	1.03E-4	0.5	4.30	1.520	0.366	0.025	2.59	1.64
Sandy loam	0.6	4.42E-6	0.5	2.49	1.17	0.392	0.01	2.69	1.64
Clay	0.2	1.44E-6	0.5	1.98	1.086	0.481	0.010	2.80	1.45

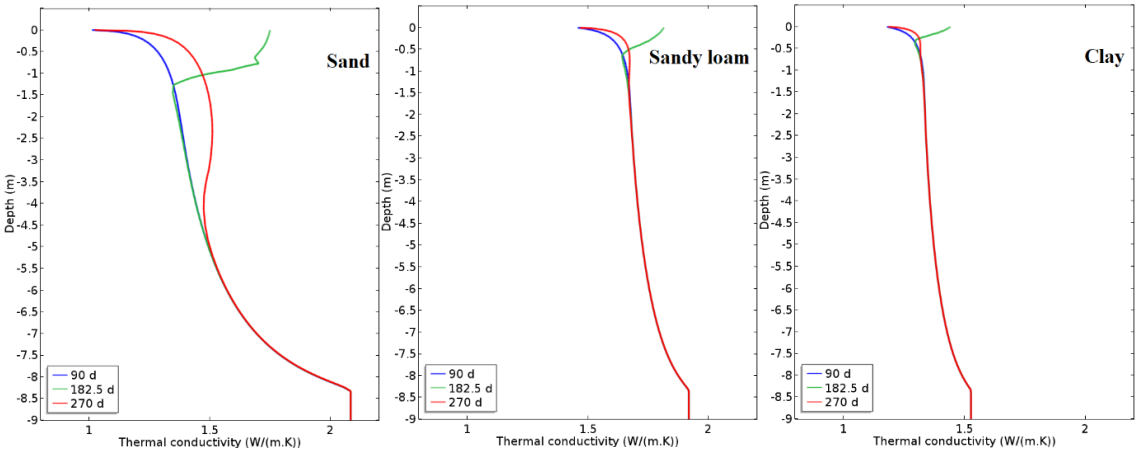

Figure 4: The thermal conductivity of three soils with time: (a) sand; (b) sandy loam; (c) clay.

REFERENCES

Abu-Hamdeh, N. and Reeder, R.: Soil thermal conductivity: effects of density, moisture, salt concentration, and organic matter, Soil Sci. Soc. Am. J., (2000), 64: 1285-1290.

Al-Khoury, R., Kolbel, T. and Schramedei, R.: Efficient numerical modeling of borehole heat exchangers, Computers & Geosciences, (2010), 36: 1301-1315.

Al-Khoury, R., Bonnier, P. and Brinkgreve, R.: Efficient finite element formulation for geothermal heating systems. Part I: Steady state, International journal for numerical methods in engineering, (2005), 63: 988-1013.

Bandos, T., Montero, A., Fernandez, E., Santander, J., Isidro, J., Perez, J., de Córdoba, P and Urchueguía, J.: Finite line-source model for borehole heat exchangers: effect of vertical temperature variations, Geothermics, (2009), 38(2): 263-70. 2009.

Bidarmaghz, A., Narsilio, G., Johnston, I. and Colls, S.: The importance of surface air temperature fluctuations on long-term performance of vertical ground heat exchangers, Geomechanics for Energy and the Environment, (2016), 6: 35-44.

Carslaw, H. and Jaeger, J.: Conduct of heat in solids (2nd edition) Oxford University Press, Lundon, UK, (1959).

Casasso, A. and Sethi, R.: Efficiency of closed loop geothermal heat pumps: a sensitivity analysis, Renew. Energy., (2014), 62:737-746.

Claesson, J. and Eskilson, P.: Conductive heat extraction to a deep borehole - thermal analyses and dimensioning rules, Energy, (1988), 13: 509-27.

Cui, W., Gawecka, K., Potts, D., Taborda, D. and Zdravkovi, W.: Numerical analysis of coupled thermo-hydraulic problems in geotechnical engineering, Geomechanics for Energy and the Environment, (2016), 6:22-34.

Florides G. and Kalogirou S.: Ground heat exchangers-A review of systems, models and applications, Renewable Energy, (2007), 32: 2461-2478.

Glen Dimplex Deutschland GmbH, Heat pump SI30TER+, Equipment data, (2016), http://www.dimplex.de/pdf/de/produktattribute/produkt_1722822_extern _egd.pdf.

Hein, P., Kolditz, O., Gorke, U., Bucher, A. and Shao, H. A numerical study on the sustainability and efficiency of borehole heat exchanger coupled ground source heat pump systems, Applied Thermal Engineering, (2016), 100: 421-433.

Hu, J.: An improved analytical model for vertical borehole ground heat changer with multiple-layer substrates and groundwater flow, Applied Energy, (2017), 202: 537-549.

Javed, S. and Spitler, J.: Accuracy of borehole thermal resistance calculation methods for grouted single U-tube ground heat exchangers, Applied Energy, (2017), 187: 790-806.

Lamarche, L. and Beauchamp, B.: New solutions for the short-time analysis of geothermal vertical boreholes, International Journal of Heat and Mass Transfer, (2007), 50: 1408-1419.

Lee, C. and Lam H. Computer simulation of borehole ground heat exchangers for geothermal heat pump systems, Renewable Energy, (2008), 33: 1286-1296.

Marcotte, D., Pasquier, P., Sheriff, F. and Bernier, M.: The importance of axial effects for borehole design of geothermal heat-pump systems, Renewable Energy, (2010), 35: 763-770.

Mikhaylova, O., Johnston, I. and Narsilio, G.: Uncertainties in the design of ground heat exchangers, Environmental Geotechnics, (2016) 3: 253 - 264.

Molina-Giraldo, N., Blum, P., Zhu, K., Bayer, P. and Fang, Z.: A moving finite line source model to simulate borehole heat exchangers with groundwater advection, International Journal of Thermal Sciences, (2011), 50:2506-2513.

Mualem, Y.: A new model for predicting the hydraulic conductivity of unsaturated porous media, Water Resour. Res., (1976) 12(3): 513-522.

Nowamooz, H., Nikoosokhan, S., Lin, J. and Chazallon, C.: Finite difference modeling of heat distribution in multilayer soils with time-spatial hydrothermal properties, Renewable Energy, (2015), 76:7-15.

Radioti G., Sartor, K., Charlier R., Dewallef, P. and Nguyen F.: Effect of undisturbed ground temperature on the design of closed-loop geothermal systems: A case study in a semi-urban environment, Applied Energy, (2017), 200: 89-105.

Richards, L.: Capillary conduction of liquids through porous mediums, J. Appl. Phys., (1931), 1: 318-333.

Rivera, J., Blum, P. and Bayer P. Ground energy balance for borehole heat exchangers: Vertical fluxes, groundwater and storage, Renewable Energy, (2015), 83: 1341-1351.

Sanner, B., Karytsas, C., Mendrinos, D. and Rybach, L.: Current status of ground source heat pumps and underground thermal energy storage in Europe, Geothermics, (2003), 32 (4): 579-588.

Saner, D., Juraske, R., Kübert, M., Blum, P., Hellweg, S. and Bayer, P.: Is it only CO2 that matters? A life cycle perspective on shallow geothermal systems, Renew Sustain Energy Rev, (2010), 14:1798-813.

Shao, H., Hein, P., Sachse and A., Kolditz, O.: Geoenergy Modeling II: Shallow Geothermal Systems, Springer briefs in energy: computational modeling of energy systems, (2016).

Sliwa, T. and Rosen, M.: Natural and Artificial Methods for Regeneration of Heat Resources for Borehole Heat Exchangers to Enhance the Sustainability of Underground Thermal Storages: A Review, Sustainability, (2015), 7: 13104-13125.

Tang, F. and Nowamooz, H.: Long-term performance of a Shallow Borehole Heat Exchanger installed in a geothermal field of Alsace region, Renewable Energy, (2018), 128: 210-222.

Tang, F. and Nowamooz, H.: Factors influencing the performance of shallow Borehole Heat Exchanger, Energy Conversion and Management, (2019), 181:571-583.

van Genuchten, M.: A closed-form equation for predicting the hydraulic conductivity of unsaturated soils, Soil Sci. Soc. Am. J., (1980), 44, 892-898.

Liu, J., Wang, F., Cai, W., Wang, Z., Wei, Q. and Deng, J.: Numerical study on the effects of design parameters on the heat transfer performance of coaxial deep borehole heat exchanger, International Journal of Energy Research, (2019), 1-16.

Wilson, G., Fredlund, D. and Barbour, S.: The effect of soil suction on evaporative fluxes from soil surfaces, Canadian Geotechnical Journal, (1997), 34 (1): 145-155.

Zeng, H., Diao, N. and Fang, Z.: Heat transfer analysis of boreholes in vertical ground heat exchangers, International Journal of Heat and Mass Transfer, (2003), 46: 4467-4481.

Zhang, C., Hu, S., Liu, Y. and Wang Q.: Optimal design of borehole heat exchangers based on hourly load simulation, Energy, (2016) 116: 1180-1190.